IEEE Access
Multidisciplinary | Rapid Review | Open Access Journal

Date of publication xxxx 00, 0000, date of current version xxxx 00, 0000.

Digital Object Identifier 10.1109/ACCESS.2017.DOI

Finite-Time Control for Piezoelectric Actuators with a High-Order Terminal Sliding Mode Enhanced Hysteresis Observer

XIN CHE[1,2,3], (Student Member, IEEE), DAPENG TIAN[1,2,3], (SENIOR MEMBER, IEEE), RUI XU[1,3], (MEMBER, IEEE), AND PING JIA.[1,3]

[1]Changchun Institute of Optics, Fine Mechanics and Physics, Chinese Academy of Sciences, Changchun 130033, China
[2]University of Chinese Academy of Sciences, Beijing 100049, China
[3]Key Laboratory of Airborne Optical Imaging and Measurement, Chinese Academy of Sciences, Changchun 130033, China

Corresponding author: Dapeng Tian (e-mail: d.tian@ciomp.ac.cn).

This work was supported in part by the National Science Foundation of China under grant number 61673365, in part by the Youth Innovation Promotion Association of Chinese Academy of Sciences under grant number 2017257, in part by the Basic Frontier Scientific Research Plan 0-1 Original Innovation Project of the Chinese Academy of Sciences under grant number ZDBS-LY-JSC044 and in part by China Postdoctoral Science Foundation under Grant No. 2020TQ0350.

ABSTRACT Piezoelectric actuators (PZTs) are essential elements in high-precision systems. However, the hysteresis nonlinearity introduced by PZTs degrades the control accuracy. In this paper, a high-order terminal sliding mode enhanced hysteresis observer is designed, which compensates the error between the Bouc-Wen model and the actual hysteresis. Subsequently, a novel terminal sliding mode control (TSMC) is proposed. Unlike the conventional TSMC, the novel TSMC method makes the tracking error in the sliding mode converge to the origin within a finite time regardless of the initial conditions, which improves the performance of conventional TSMC. The stability of the proposed control method is verified through the Lyapunov theory. Finally, simulations and experiments are implemented to validate the effectiveness of the proposed control method. Experimental results demonstrate that the proposed method has a more superior performance than conventional TSMC.

INDEX TERMS Piezoelectric actuator, hysteresis, terminal sliding mode control, observer.

I. INTRODUCTION

PIEZOELECTRIC actuators (PZTs) have become one of the key components in various precision engineering applications, such as atomic force microscopy [1], tilting mirrors [2], biological micromanipulation [3], and high-precision manufacturing machines [4]. The reason lies in the fact that PZT provides the advantage of ultrahigh resolution, high stiffness, rapid response, and large output force [5]. However, the PZT introduces nonlinear effect into the system, which is mainly attributed to hysteresis. The hysteresis is a nonlinear relationship between the applied voltage and the output displacement of PZT, which induces a severe open-loop positioning error as much as 15% of the travel range [6]. Therefore, it is essential to overcome the hysteresis nonlinearity to achieve a high precision control for a PZT driven motion system [7].

Various control strategies have been proposed to coupe with this problem, which can be generally classified into two categories in terms of hyteresis model-based feedforward control and hyteresis model-free feedback control [6]. The feedforward controller can compensate the hysteresis effect by cascading an inverse hysteresis model. For instance, hysteresis identifications using Preisach model [8], Prandtl–Ishlinskii model [9], Duhem model [10], and Bouc–Wen model [11], etc., have been widely carried out. As an analytical model, the Bouc–Wen model possesses the advantage of computational simplicity because only one nonlinear differential equation is used to describe the hysteresis loop [12]. However, the Bouc-Wen model are effective to describe the rate-independent hysteresis. As a matter of fact, the hysteresis effect of PZTs is rate-dependent [13]. Besides, the open-loop controller is sensitive to the modeling accuracy.

This article has been accepted for publication in a future issue of this journal, but has not been fully edited. Content may change prior to final publication. Citation information: DOI 10.1109/ACCESS.2020.3044188, IEEE Access

An error always exists between the hysteresis model and the actual hysteresis of the PZT system.

In contrast, the robust feedback control, which considers the piezoelectric nonlinearity as an unmodelled disturbance to a nominal model. Various types of robust controllers have been developed to tackle the hysteretic nonlinearity, such as H_∞ control [14], adaptive control [15], intelligent control [16], [17], sliding mode control (SMC) [18], and so on. Among these methods, SMC has been proven to be an effective method to maintain the system stability and consistent performance in the presence of parameter perturbations and disturbances [19]. In [20], an adaptive SMC is designed to deal with the uncertainties of Markov jump systems with actuator faults. In addition, there is no need to establish the hysteresis inverse model when using SMC in PZT system [21]. The control structure is simple and clear.

However, the convergence rates of conventional linear sliding surface can only ensure exponential with infinite settling time [22]. Finite-time control method have attracted much attention because finite-time convergence usually demonstrates faster convergence rates and stronger robustness, such as finite-time state feedback control [23], [24], finite-time convergent observer design [25], [26] and finite-time output feedback control [27], [28], etc. Terminal sliding mode control (TSMC) method with a nonlinear sliding surface combines the finite-time method and SMC together, which can guarantee that the states converge to the origin in finite time [29]. Nice features such as better disturbance rejection properties and robustness are brought into the system as a result of finite-time convergence [30]. Additional, non-singular TSMC [31] has been developed to avoid the singularity of TSMC.

Moreover, the robustness of SMC can normally be obtained by the selection of a large switching gain, which will cause undesired chattering phenomenon [32]. The boundary layer method is usually used to reduce chattering of SMC and the method suppressed the hysteresis effect in the piezo-actuated stages effectively [33]. High-order terminal sliding mode is also an effective way to reduce chattering. In [34], a new continuous third-order sliding mode control scheme is proposed and achieves remarkable robust tracking performance for piezoelectric-driven motion system.

It is worth noting that the settling time of TSMC is a function of the initial conditions of the system [35]. In general, different initial values lead to different estimations of convergence time. Moreover, it is difficult to obtain the initial conditions of the actual system accurately in advance, which makes settling time inaccessible and deteriorates the performance of the system. In order to solve the problem, a novel terminal sliding mode control scheme is designed of which the convergence time is independent of the initial state of the error. However, only using the controller, the disturbance rejection performance of the system is still limited. Therefore, a high-order terminal sliding mode enhanced hysteresis observer which compensates the error between the hysteresis model and the actual hysteresis is devised in this paper to improve the control accuracy of the PZT system. Different from the traditional disturbance observer, the high-order terminal sliding mode enhanced hysteresis observer is based on Bouc-Wen model to solve the problem of hysteresis observation. The primary contributions of this work are briefly outlined as follows:

1) A high-order terminal sliding mode enhanced hysteresis observer is designed, which compensates the error between the Bouc-Wen model and the actual hysteresis using high-order terminal sliding mode. Thus, the precision of the hysteresis estimation is improved. Besides, the chattering of high-order terminal sliding mode is reduced using an integral function;
2) A novel terminal sliding mode surface is proposed, which not only can provide a finite-time convergence, but also makes the tracking error in the sliding mode converge to the origin within a maximum settling time regardless of the initial conditions;
3) The stability of the combined controller is analyzed using the Lyapunov stability theory; and the tracking performance of the resulting control system as compared to that of the conventional TSMC and the novel TSMC is demonstrated by experimental investigations on a PZT driven tip/tilt platform.

The remainder of this paper is organized as follows. Section II describes the Bouc-Wen model of the PZT. Section III introduces the conventional TSMC method. Section IV provides the design process of the novel TSMC based on high-order terminal sliding mode enhanced hysteresis observer, and the stability analysis is proved by the Lyapunov theory. Section V provides the simulation results which verify the effectiveness of the proposed controller. Section VI gives the comparison experimental results of the proposed controller and other control methods. Finally, Section VII provides the conclusions of this paper.

II. DESCRIPTION AND IDENTIFICATION OF THE BOUC-WEN MODEL

The hysteresis effect of PZT system can be expressed using the following static Bouc-Wen model [36]

$$\begin{cases} \dot{x} = a_0 x + a_1 u + a_2 h + d \\ \dot{h} = \alpha \dot{u} - \beta |\dot{u}| h |h|^{n-1} - \gamma \dot{u} |h|^n \end{cases} \tag{1}$$

where x denotes the output displacement of the PZT system, u is the input voltage, a_0, a_1 and a_2 represent the nominal parameters of the system, h denotes the hysteresis term of the Bouc-Wen model, the coefficients α, β and γ determine the amplitude and shape of the Bouc-Wen model respectively, d represents the unknown external disturbances of the system and n governs the smoothness of the transition from elastic to plastic response. For the elastic structure and material, $n = 1$ is assigned in (1) as usual.

Due to the complexity of Bouc-Wen model, it is difficult to identify the parameters of the parameters using conventional approaches [37]. In this study, the bat-inspired optimization

This article has been accepted for publication in a future issue of this journal, but has not been fully edited. Content may change prior to final publication. Citation information: DOI 10.1109/ACCESS.2020.3044188, IEEE Access

TABLE 1. Identified model parameters of the PZT with Bouc-Wen hysteresis.

Parameters	Value	Units
a_0	-1332	-
a_1	359	-
a_2	-1332	-
α	1.0642	$mrad/V$
β	5.2644	V^{-1}
γ	-2.3694	V^{-1}

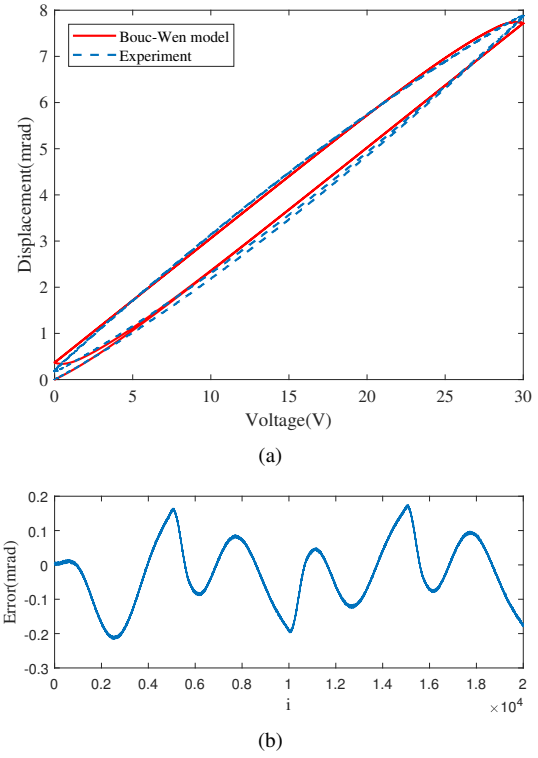

FIGURE 1. Results of the identified Bouc-Wen model. (a) Comparison of Bouc-Wen model and experimental result; (b) Prediction errors of identified Bouc-Wen model.

algorithm [38] is facilitated to identify the parameters of Bouc-Wen model (1). The bat-inspired optimization algorithm is adopted in the current problem because it possess a faster convergent rate and stronger robustness compared with the other optimization algorithms. The specific identification process can be referred in [21].

The identified model parameters are listed in Table 1, and the comparison of the obtained model and experimental results is shown in Fig. 1(a). The prediction error of the obtained model is shown in Fig. 1(b), and it can be observed that the maximum (MAX) error is 0.2164 mrad, which is 2.79% of the whole range of the PZT system.

In consideration of the parameter uncertainties, the PZT system based on Bouc-Wen model is described as

$$\begin{cases} \dot{x} = (a_0 + \delta_0)x + (a_1 + \delta_1)u + (a_2 + \delta_2)h + d \\ \dot{h} = \alpha\dot{u} - \beta|\dot{u}|h - \gamma\dot{u}|h| \end{cases} \tag{2}$$

where δ_0, δ_1 and δ_2 are the uncertain parameters parts, $\Phi = \delta_0 x + \delta_1 u + \delta_2 h + d$ represents the lumped disturbance caused by the external noise, parameter uncertainties, which is bounded and satisfies $|\Phi| \leq \Phi_0$, where Φ_0 is a positive constant.

The control problem becomes how to achieve a precision tracking of the motion trajectory x_d in the presence of the lumped disturbance Φ. In order to achieve a precision motion control, a robust control scheme is devised in Section IV.

III. CONVENTIONAL TSMC DESIGN

In this section, a conventional TSMC method is introduced to eliminate hysteresis of the PZTs. At first, the tracking error is defined as follows

$$e = x_d - x \tag{3}$$

where x_d is the desired displacement of the PZT system. A terminal sliding mode surface [39] is designed as

$$\sigma = e + \lambda \int_0^t \text{sig}^p(e(\tau))\text{d}\tau \tag{4}$$

where $\lambda > 0, 0 < p < 1$ are positive constants, $\text{sig}^p(x) = |x|^p \text{sign}(x)$ is introduced in the following analysis for simplicity of expression.

The conventional TSMC is designed as

$$u = \frac{1}{a_1}(\dot{x}_d - a_0 x - a_2 h + \lambda \text{sig}^p(e) + k\text{sig}^\epsilon(\sigma)) \tag{5}$$

where $k > 0$ and $0 < \epsilon < 1$ are constants to be designed.

Theorem 1: For system (1), under control law (5), the tracking error can convergence to zero in finite time.

Lemma 1 [40]: Consider the nonlinear system $\dot{x} = f(x, u),\ f(0) = 0, x \in R^n$, where x is a state vector, u is the input vector. Suppose that there exist $\kappa > 0, 0 < \rho < 1$ and $0 < \Delta < \infty$ such that the continuous function $V(x)$ satisfies

$$\dot{V}(x) \leq -\kappa V^\rho(x) + \Delta. \tag{6}$$

Then, the trajectory of system is practical finite time stable. The reaching time is bounded by

$$t \leq \frac{V^{1-\rho}(x(0))}{\kappa\kappa_0(1-\rho)} \tag{7}$$

where $0 < \kappa_0 < 1$, and $V(x(0))$ is the initial value of $V(x)$.

Proof: Choosing Lyapunov function as

$$V = \frac{1}{2}\sigma^2 \tag{8}$$

By taking the time derivative of (8) gains

$$\begin{aligned} \dot{V} &= \sigma\dot{\sigma} = \sigma(\dot{e} + \lambda \text{sig}^p(e)) \\ &= \sigma(\dot{x}_d - a_0 x - a_1 u - a_2 h - \Phi + \lambda \text{sig}^p(e)) \end{aligned} \tag{9}$$

Substituting (5) into (9) yields

$$\begin{aligned} \dot{V} &= \sigma(\dot{x}_d - a_0 x - a_2 h - \Phi + \lambda \text{sig}^p(e) \\ &\quad - (\dot{x}_d - a_0 x - a_2 h + \lambda \text{sig}^p(e) + k\text{sig}^\epsilon(\sigma))) \\ &= -k|\sigma|^{\epsilon+1} - \sigma\Phi \\ &\leq -2^{\frac{\epsilon+1}{2}} k V^{\frac{\epsilon+1}{2}} + |\sigma|\Phi_0 \end{aligned} \tag{10}$$

This article has been accepted for publication in a future issue of this journal, but has not been fully edited. Content may change prior to final publication. Citation information: DOI 10.1109/ACCESS.2020.3044188, IEEE Access

According to Lemma 1, the TSMC manifold $\sigma(t) = 0$ can be reached in finite time, then, we have

$$\dot{e} = -\lambda \text{sig}^p(e) \tag{11}$$

Thus, the convergence time is obtained as

$$t_f = \frac{|e(0)|^{1-p}}{\lambda(1-p)} \tag{12}$$

Hence, the error can convergence to zero in finite time. □

Remark 1: It notes that the error can convergence to zero in finite time, which is dependent on the initial value of error. It is hard to obtain the initial conditions of the actual system accurately in advance, which makes the settling time of the system difficult to achieve and degrades the control precision.

To this end, a novel terminal sliding mode surface is proposed in Section IV, which not only can provide a finite-time convergence, but also makes the tracking error in the sliding mode converge to the origin within a maximum settling time regardless of the initial conditions. By selecting appropriate parameters, the convergence rate of system error can be improved, and then the performance of the system can be enhanced.

IV. PROPOSED CONTROLLER DESIGN

A. HYSTERESIS OBSERVER DESIGN

Although the Bouc-Wen model is effective to describe the rate-independent hysteresis, the hysteresis effect of PZTs is rate-dependent, an error between the identification and the practice of the hysteresis model always exists. To this end, a high-order terminal sliding mode enhanced hysteresis observer is designed in the following subsection.

Define $f(u,h) = \beta|\dot{u}|h + \gamma\dot{u}|h|$. Equation (1) can be rewritten as

$$\begin{cases} \dot{x} = a_0 x + a_1 u + a_2 h \\ \dot{h} = \alpha\dot{u} - f(u,h) \end{cases} \tag{13}$$

The high-order terminal sliding mode enhanced hyteresis observer is designed as

$$\begin{cases} \dot{\hat{x}} = a_0\hat{x} + a_1 u + a_2\hat{h} + u_{tsmo1} \\ \dot{\hat{h}} = \alpha\dot{u} - f(u,\hat{h}) + u_{tsmo2} \end{cases} \tag{14}$$

where $\hat{x}$ represents the estimated value of the displacement, u_{tsmo1} and u_{tsmo2} represents the designed control law. The displacement estimated error $\tilde{x}$ and system hyteresis estimated error $\tilde{h}$ are defined as $\tilde{x} = x - \hat{x}$, $\tilde{h} = h - \hat{h}$. Besides, $\tilde{f}(u,h,\hat{h}) = f(u,h) - f(u,\hat{h})$. It can be concluded from [41] that h is bounded and satisfies $|h| \le h_0$, where h_0 is a positive constant. In the meantime, the derivative of the control input u is bounded for a practical system, satisfying $|\dot{u}| \le w$, where w is a positive constant. So it is reasonable to assume that $\tilde{f}$ is bounded and satisfies $\tilde{f} \le (|\beta| + |\gamma|)w(|h_0| + |\hat{h}|)$. Then, the error dynamics becomes

$$\dot{\tilde{x}} = a_0\tilde{x} + a_2\tilde{h} - u_{tsmo1} \tag{15a}$$

$$\dot{\tilde{h}} = -\tilde{f} - u_{tsmo2} \tag{15b}$$

A fast terminal sliding surface is designed as follows,

$$\sigma_h = \dot{\tilde{x}} + \zeta\tilde{x} + \xi \text{sig}^q(\tilde{x}) \tag{16}$$

where $0 < q < 1$, ζ and ξ are positive constants to be designed.

The high-order terminal sliding mode is designed to achieve chattering-free control by shifting the discontinuous control to the derivative of the control law. The sliding mode function is designed as

$$u_{tsmo1} = (a_0 + \zeta)\tilde{x} + \xi \text{sig}^q(\tilde{x}) + v \tag{17a}$$

$$\dot{v} + T_w v = l_1 \text{sign}(\sigma_h) \tag{17b}$$

$$u_{tsmo2} = l_2 \text{sign}(\sigma_h) \tag{17c}$$

where $\sigma_h(0) = 0$, l_1 is the control gain, l_2 is the feedback gain, and $T_\omega > 0$ is the designed parameter. The observer can obtain satisfactory observation performance by appropriately adjusting the parameters l_1, l_2, and T_ω.

Theorem 2: For error system (15), if $l_1 > |T_\omega v|$ and $l_2 > |\tilde{f}|$ holds, under control law (17), the error state $\tilde{x}$ and $\dot{\tilde{x}}$ converge to zero in finite time.

Proof: The sliding surface σ_h can be written by substituting (15a) and (17a) into (16),

$$\sigma_h = a_2\tilde{h} - v \tag{18}$$

The derivative of σ_h with respect to time t by combining (17b) and (17c) can be expressed as follows

$$\begin{aligned} \dot{\sigma}_h &= a_2\dot{\tilde{h}} - \dot{v} \\ &= -\tilde{f} - u_{smo2} + T_w v - l_1 \text{sign}(\sigma_h) \\ &= -\tilde{f} - l_2 \text{sign}(\sigma_h) + T_w v - l_1 \text{sign}(\sigma_h) \end{aligned} \tag{19}$$

Define Lyapunov function

$$V_h = \frac{1}{2}\sigma_h^2 \tag{20}$$

By selecting $l_1 > |T_\omega v|$ and $l_2 > |\tilde{f}|$, according to (19), the derivative of V_h with respect to time t yields,

$$\begin{aligned} \dot{V} &= \sigma_h\dot{\sigma}_h \\ &= \sigma_h(-\tilde{f} - l_2 \text{sign}(\sigma_h) + T_w v - l_1 \text{sign}(\sigma_h)) \\ &= -\tilde{f}\sigma_h - l_2|\sigma_h| + T_w v\sigma_h - l_1|\sigma_h| < 0 \end{aligned} \tag{21}$$

Therefore, the system dynamics can converge to the fast terminal sliding surface (16) within finite time. Then, the following equation holds,

$$\sigma_h = \dot{\tilde{x}} + \zeta\tilde{x} + \xi \text{sig}^q(\tilde{x}) = 0 \tag{22}$$

By solving the above equation, the exact time to reach $\tilde{x} = 0$ can be calculated as

$$t_h = \frac{1}{\zeta(1-q)} \ln \frac{\zeta|e(0)|^{1-q} + \xi}{q} \tag{23}$$

Therefore, the state $\tilde{x}$ and $\dot{\tilde{x}}$ can converge to zero in finite time. □

This article has been accepted for publication in a future issue of this journal, but has not been fully edited. Content may change prior to final publication. Citation information: DOI 10.1109/ACCESS.2020.3044188, IEEE Access

Remark 2: Convergence of $\tilde{h}$: By applying $\sigma_h = 0$ in (17b), we can obtain

$$v = Ce^{-T_w t}. \tag{24}$$

By substituting (24) into (18), we can obtain

$$\tilde{h} = \frac{1}{a_2} Ce^{-T_w t}. \tag{25}$$

To guarantee the convergence of hysteresis estimation error $\tilde{h}$, the control parameter should be selected as $T_w > 0$. And the convergence rate of $\tilde{h}$ can be optimized by adjusting T_w.

Remark 3: Chattering Suppression Analysis: The chattering suppression of the proposed high-order terminal sliding mode enhanced hysteresis observer is analyzed. From (17a) and (17b), it can be concluded that the chattering signal $l_1 \text{sign}(\sigma_h)$ is smoothed by an equivalent low-pass filter. The transfer function from $l_1 \text{sign}(\sigma_h)$ to v can be expressed as

$$G(s) = \frac{1}{s + T_\omega}. \tag{26}$$

where T_ω represents the bandwidth of the low-pass filter. Therefore, the proposed observer possesses smooth disturbance observation.

B. NOVEL TSMC DESIGN

A novel TSMC is designed in the following subsection, which can provide a finite-time convergence independent on the initial value of error.

The novel TSMC surface is defined as

$$\sigma = e + \int_0^t [\lambda_1 \text{sig}^{1+\frac{1}{\mu}}(e) + \lambda_2 \text{sig}^{1-\frac{1}{\mu}}(e)] \text{d}\tau \tag{27}$$

where $\mu > 1, \lambda_1, \lambda_2 > 0$ are parameters to be designed.

Based on the sliding surface (27), the novel TSM controller is designed as

$$\begin{aligned} u = &\frac{1}{a_1}(\dot{x}_d - a_0 x - a_2 h + \lambda_1 \text{sig}^{1+\frac{1}{\mu}}(e) \\ &+ \lambda_2 \text{sig}^{1-\frac{1}{\mu}}(e) + k_1 \text{sig}^{\epsilon}(\sigma) + k_2 \sigma). \end{aligned} \tag{28}$$

where $k_1, k_2 > 0$ and $0 < \epsilon < 1$ are constants to be designed.

Theorem 3: For system (1), under control law (28), the error can convergence to zero in a finite time, which is independent on the initial value of the error.

Proof: Define Lyapunov function as

$$V = \frac{1}{2}\sigma^2 \tag{29}$$

Its differential with respect to time is

$$\begin{aligned} \dot{V} &= \sigma\dot{\sigma} = \sigma(\dot{e} + \lambda_1 \text{sig}^{1+\frac{1}{\mu}}(e) + \lambda_2 \text{sig}^{1-\frac{1}{\mu}}(e)) \\ &= \sigma(\dot{x}_d - a_0 x - a_1 u - a_2 h - \Phi \\ &+ \lambda_1 \text{sig}^{1+\frac{1}{\mu}}(e) + \lambda_2 \text{sig}^{1-\frac{1}{\mu}}(e)) \end{aligned} \tag{30}$$

Substituting (28) into (30) yields

$$\begin{aligned} \dot{V} &= \sigma(\dot{x}_d - a_0 x - a_2 h - \Phi + \lambda_1 \text{sig}^{1+\frac{1}{\mu}}(e) + \lambda_2 \text{sig}^{1-\frac{1}{\mu}}(e) \\ &- (\dot{x}_d - a_0 x - a_2 h + \lambda_1 \text{sig}^{1+\frac{1}{\mu}}(e) + \lambda_2 \text{sig}^{1-\frac{1}{\mu}}(e) \\ &+ k_1 \text{sig}^{\epsilon}(\sigma) + k_2 \sigma)) \\ &= -k_1 |\sigma|^{\epsilon+1} - k_2 \sigma^2 - \sigma\Phi \\ &\le -2^{\frac{\epsilon+1}{2}} k_1 V^{\frac{\epsilon+1}{2}} + |\sigma|\Phi_0 \end{aligned} \tag{31}$$

According to Lemma 1, the tracking error reaches the sliding surface in finite time, then, we have $\dot{\sigma} = 0$. Then the sliding mode dynamics is derived as follows

$$\dot{\sigma} = \dot{e} + \lambda_1 \text{sig}^{1+\frac{1}{\mu}}(e) + \lambda_2 \text{sig}^{1-\frac{1}{\mu}}(e) = 0 \tag{32}$$

The settling time of (32) is determined by

$$t_l = \int_0^{|e(0)|} \frac{\text{d}e}{\lambda_1 e^{1+\frac{1}{\mu}} + \lambda_2 e^{1-\frac{1}{\mu}}}. \tag{33}$$

We choose an alternate variable $z = e^{\frac{1}{\mu}}$, Then, we obtain

$$\begin{aligned} t_l &= \int_0^{|e(0)|^{\frac{1}{\mu}}} \frac{\mu z^{\mu-1} \text{d}z}{\lambda_1 z^{\mu+1} + \lambda_2 z^{\mu-1}} \\ &= \mu \int_0^{|e(0)|^{\frac{1}{\mu}}} \frac{\text{d}z}{\lambda_1 z^2 + \lambda_2 z} \\ &= \frac{\mu}{\sqrt{\lambda_1 \lambda_2}} \arctan(\sqrt{\frac{\lambda_1}{\lambda_2}} |e(0)|^{\frac{1}{\mu}}) \\ &\le \frac{\pi\mu}{2\sqrt{\lambda_1 \lambda_2}} \end{aligned} \tag{34}$$

Therefore, the tracking error can reach the origin in a maximum settling time, which is independent of initial state $e(0)$. □

Remark 4: It can be implied from (34) that a smaller μ and larger λ_1 and λ_2 provide a shorter settling time, which implies a faster response speed and higher tracking accuracy. However, this will amplify the measurement noise in the actual system.

If the observed hysteresis is taken into consideration, the controller can be modified as

$$\begin{aligned} u = &\frac{1}{a_1}(\dot{x}_d - a_0 x + \lambda_1 \text{sig}^{1+\frac{1}{\mu}}(e) + \lambda_2 \text{sig}^{1-\frac{1}{\mu}}(e) \\ &+ k_1 \text{sig}^{\epsilon}(\sigma) + k_2 \sigma - a_2 \hat{h}). \end{aligned} \tag{35}$$

The block diagram of the proposed controller is illustrated in Fig. 2.

Remark 5: Boundary layer method [42] is employed to smooth the control signal. The saturation function (36) is adopted to replace the signum function to decrease the chattering of the signum function.

$$\text{sat}(\sigma) = \begin{cases} 1 & \sigma > \Delta \\ \sigma/\Delta & |\sigma| < \Delta \\ -1 & \sigma < -\Delta \end{cases} \tag{36}$$

where $\Delta > 0$ is the thickness of the boundary layer. Outside the boundary layer, the control is identical to the ideal switching characteristic. Within the boundary layer, the continuous

This article has been accepted for publication in a future issue of this journal, but has not been fully edited. Content may change prior to final publication. Citation information: DOI 10.1109/ACCESS.2020.3044188, IEEE Access

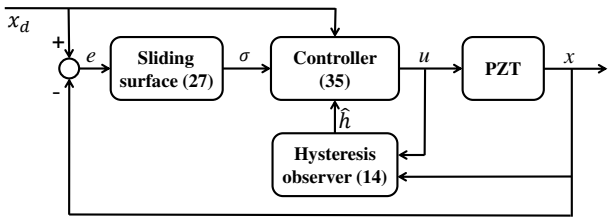

FIGURE 2. Control system block diagram.

approximation of the switch function is chosen to replace the signum function, and the control law becomes the feedback control of the continuous state. The larger the thickness of the boundary layer Δ is ,the smaller the chattering is, but the control gain will decrease and the robustness of the controller is weaker. Δ is chosen as 0.1 in the subsequent experiments through trial-and-error method.

V. SIMULATION RESULTS

In this section, simulations are carried out to determine the parameters of the proposed method using Matlab/Simulink. The established hysteresis system model which includes Bouc-Wen model and linear dynamics part is used to replace the actual PZT system in the simulations. The tracking error is obtained by subtracting the model output from the desired displacement. Parameter uncertainties and white Gaussian noise are added to the system. The speed command is set as sinusoidal signal with the amplitude of 3 mrad and the frequency of 1 Hz. The simulation results of system tracking error versus the control parameters are shown in Fig. 3. It can be implied from (34) that λ_1 and λ_2 determines the decay rate of the tracking error. Thus, larger λ_1 and λ_2 provide a higher tracking accuracy as shown in Fig. 3(a). However, too large λ_1 and λ_2 have limited improvement on the tracking accuracy, and noise is introduced into the system. Similarly, a smaller value of μ results in a smaller convergence time as seen in (34), which implies smaller tracking error as seen in Fig. 3(b); however, this will amplify the measurement noises. The choice of k_1 and ϵ requires a tradeoff between system robustness and chattering. From Fig. 3(c), a larger k_1 can improve the control accuracy, but too large k_1 will make the system chatter. Analogously, k_2 increases the stiffness of the closed-loop system, and a large k_2 injects excess noise into the system.

VI. EXPERIMENTAL RESULTS

A. EXPERIMENTAL SETUP

The experimental setup is depicted in Fig. 4. The platform is driven by a PZT with the tip/tilt angle stroke of 10 mrad (model: S-330.8SL, from Physik Instrumente Co., Ltd.). The integrated controller (model: Namiway, E-P04.2S0/10D, from Physik Instrumente Co., Ltd.) is composed of an electric strain gauge sensor and a high-voltage amplifier. A real-time controller (model: HRT1000, from HwaCreate Co., Ltd.) with 16-bit AD and DA converters is adopted as control

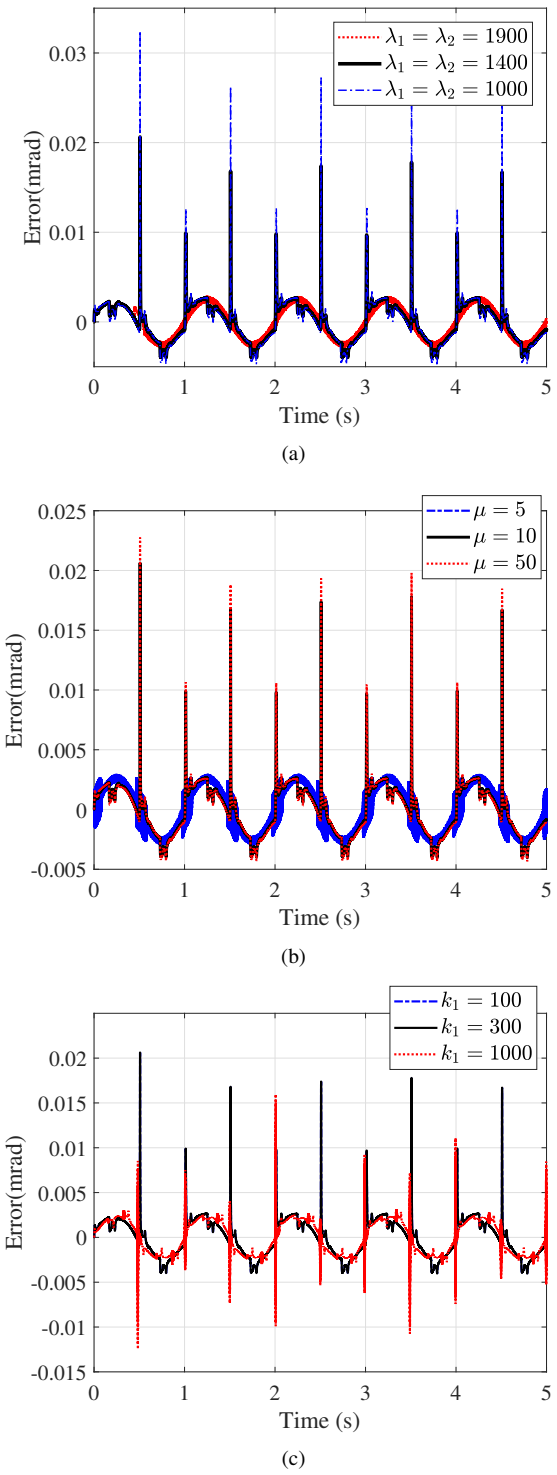

FIGURE 3. Simulation results of system tracking error versus the control parameters. (a) Error versus the parameter λ_1, λ_2; (b) Error versus the parameter μ (c) Error versus the parameter k_1, k_2, ϵ.

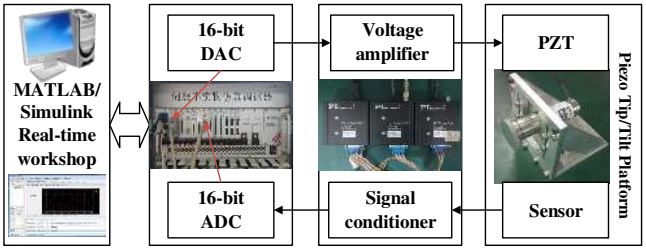

FIGURE 4. Experimental setup of a tip/tilt platform driven by a PZT.

TABLE 2. Control parameters of the developed controllers

C-TSMC (5)	TSMC (28)	Proposed (35)
$\lambda = 2800$	$\lambda_1 = 1400$	$\lambda_1 = 1400$
	$\lambda_2 = 1400$	$\lambda_2 = 1400$
$k = 300$	$k_1 = 300$	$k_1 = 300$
	$k_2 = 150$	$k_2 = 150$
$p = 0.9$	$\mu = 10$	$\mu = 10$
$\epsilon = 0.9$	$\epsilon = 0.9$	$\epsilon = 0.9$
-	-	$l_1 = 0.25$
-	-	$l_2 = 1$
-	-	$q = 0.7$
-	-	$\zeta = 0.1$
-	-	$\xi = 0.05$

hardware. The DA channel produces a voltage control signal, which is then amplified ten times via the high voltage amplifier to provide a voltage ranging from -20 to 120V for driving the PZT. In addition, the output signals of the two capacitive sensors are processed by the signal conditioner module, which produces analog voltages ranging between 0 and 10V and then acquired by the AD channel. A personal computer with Matlab/Simulink is used to implement real-time control of the tip/tilt platform system. The experiments are conducted with a sampling frequency of 5kHz. Owing to the motion decoupling in the two working axes, only one axial motion of the system is employed for the control validation in this paper.

B. EXPERIMENTAL TESTING RESULTS

The performance of the piezoelectric actuator system with different controllers is tested by experiments in this section. Specifically, conventional terminal sliding mode control (C-TSMC) method (5) and the novel terminal sliding mode control (TSMC) method are (28) implemented at the same time. The control parameters of the three controllers are shown in Table 2, which are tuned by trial and error method. For a fair comparison, the switching gains of the controllers are selected as the same value. With the developed controllers, several experimental studies are carried out to examine the performance.

1) Sinusoidal Motion Tracking

A sinusoidal signal with amplitude of 3 mrad and frequency of 5 Hz is tracked using the above methods. The results are shown in Fig. 5. The MAX tracking error and the root

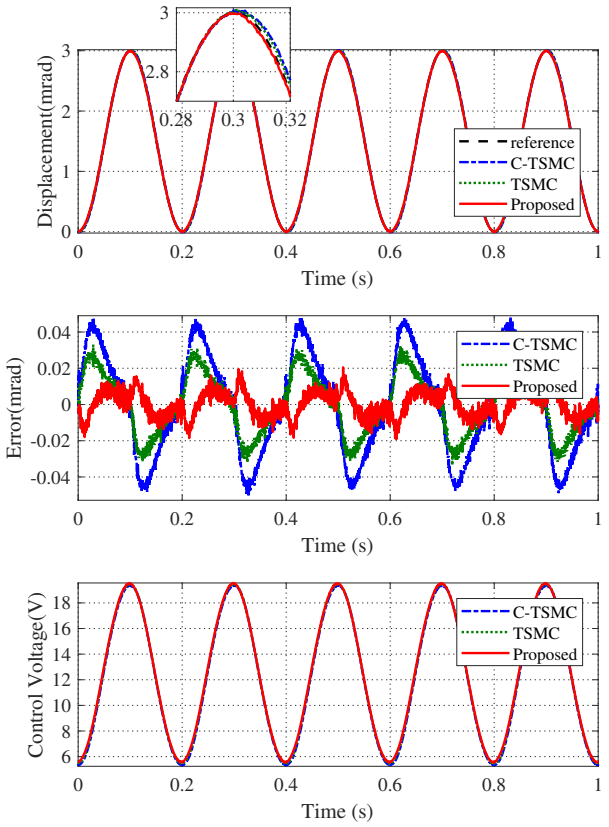

FIGURE 5. Results of sinusoidal signal motion tracking with amplitude of 3mrad and frequency of 5 Hz.

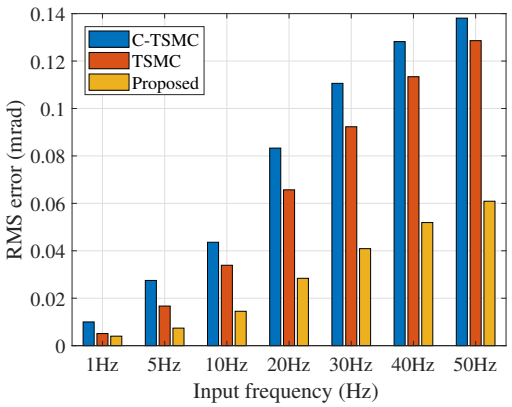

FIGURE 6. RMS tracking error versus input frequency.

mean square (RMS) error of the proposed control method are 0.0206 mrad and 0.0074 mrad, respectively. In contrast with the C-TSMC method, the proposed control method attenuates the MAX tracking error and the RMS error by 61.1% and 73.1%; compared with the TSMC method, the proposed control method reduces the MAX tracking error and the RMS error by 39.8% and 55.7%, respectively.

This article has been accepted for publication in a future issue of this journal, but has not been fully edited. Content may change prior to final publication. Citation information: DOI 10.1109/ACCESS.2020.3044188, IEEE Access

TABLE 3. Control results of triangular motion tracking

Controller	MAX error (mrad)	RMS error (mrad)
C-TSMC	0.1679	0.0238
TSMC	0.1670	0.0187
Proposed	0.0929	0.0135

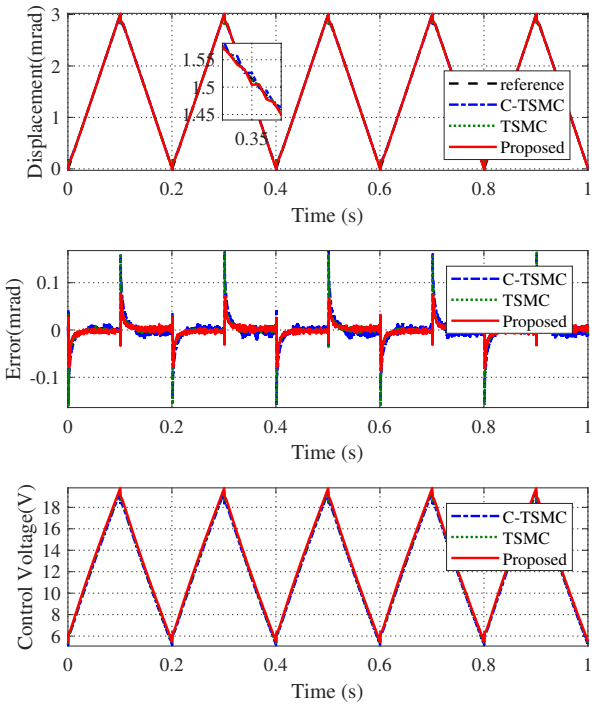

FIGURE 7. Results of triangular signal motion tracking with amplitude of 3mrad and frequency of 5 Hz.

Furthermore, a series of experiments are carried out as the frequency of the sinusoidal signal is gradually increased. As the input frequency of the sinusoidal trajectory increases from 1 Hz to 50 Hz, the RMS tracking errors of the three controllers are shown in Fig. 6 . The advantage of the proposed method compared with the other two controllers is evident for sinusoidal signal motion tracking at both low and high input frequencies.

To further verify the performance of the proposed controller, the digital sliding mode prediction control method [43] is compared with the proposed method. The digital sliding mode prediction control method produces the MAX tracking error rate of 2.17% and RMS error rate of 0.61% for a sinusoidal signals with 10 Hz. In particular, the proposed control method can alleviate the MAX tracking error and RMS error by 45.0% and 20.5%, respectively. Therefore, the proposed control method is superior to other robust control method.

TABLE 4. Control results of multi-frequency signal motion tracking

Controller	MAX error (mrad)	RMS error (mrad)
C-TSMC	0.0311	0.0147
TSMC	0.0251	0.0096
Proposed	0.0149	0.0042

2) Triangular Motion Tracking

The triangular signal with the amplitude of 3 mrad and the frequency of 5 Hz is used as the desired signal to prove the effectiveness of the proposed controller on the PZT system. The position tracking results of the triangular signal based on the three different controllers are shown in Fig. 7. The MAX tracking errors and the RMS errors are described in Table 3. It can be observed from Table 3 that, in contrast with the C-TSMC method, the proposed control method attenuates the MAX tracking error and the RMS error by 44.7% and 43.3%, respectively. Moreover, the proposed control method reduces the MAX tracking error and the RMS error by 44.4% and 27.8% in comparison with the TSMC method, respectively. It is obvious that the proposed controller can effectively eliminate the hysteresis nonlinearity of the PZT system and has the best performance in terms of the triangular signal motion tracking. In addition, compare with continuous third-order SMC [34] that achieved the RMS rate error rate of 0.75% for a triangular signal with frequency of 5Hz, the proposed control method decrease the RMS error by 40.0%. This further proves the effectiveness of the proposed method.

3) Multi-frequency Motion Tracking

To further validate the proposed approach in regulating the minor loop properties of the hysteresis effect, a multi-frequency harmonic signal $x_d = 1.8 + 1.2\sin(2\pi t - 0.5\pi) + 0.6\sin(10\pi t)$ mard was applied. The tracking results are demonstrated in Figs. 8. In Table 4, the comparative tracking results of the three controllers are listed. Compared with the C-TSMC method, the proposed control method mitigates the MAX tracking error and the RMS error by 52.1% and 71.4%, respectively; compared with the TSMC method, the MAX tracking error and the RMS error of the proposed control method decrease by 30.1% and 56.3%, respectively. Therefore, the tracking errors caused by both the major-loop and minor-loop hysteresis nonlinearities are significantly suppressed. Further, the proposed method is compared with [21] which achieved the MAX tracking error rate of 0.94% and the RMS error rate of 0.35% for a complex harmonic signal of 1Hz and 5Hz. The proposed method attenuates the MAX tracking error and the RMS error of [21] by 55.8% and 66.7%, respectively. It is clearly seen that the proposed method achieves the best suppression effect on the hysteretic nonlinearity.

VII. CONCLUSION AND FUTURE WORKS

In this paper, the hysteresis nonlinearity of the PZT is described using the Bouc-Wen. Based on the obtained Bouc-Wen model, a high-order terminal sliding mode enhanced

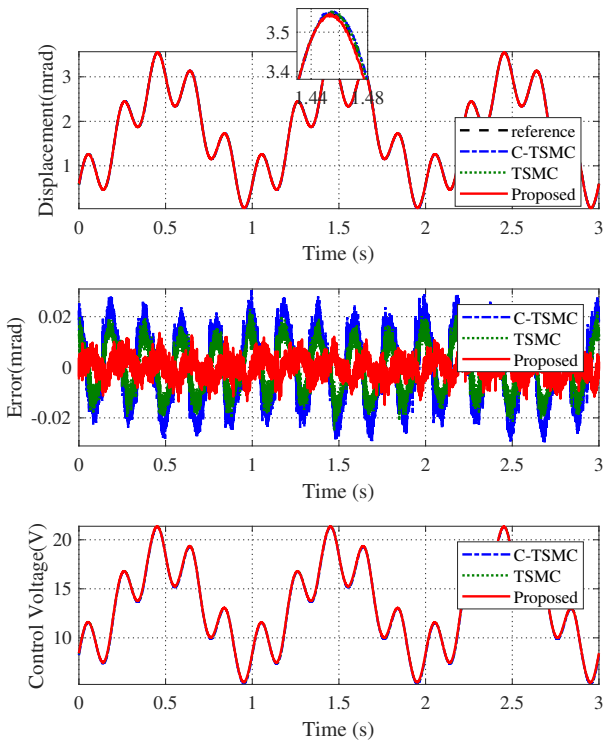

FIGURE 8. Results of multi-frequency sinusoidal signal motion tracking.

hysteresis observer is designed to compensate for the error between the identified Bouc-Wen model and the real hysteresis of the PZT system. A novel TSMC is designed which not only can provide a finite-time convergence, but also makes the tracking error in the sliding mode converge to the origin within a maximum settling time. The experimental results validate that the proposed control method can effectively suppress the hysteresis nonlinearity effect and realize the high precision tracking control of the PZT system.

Although the hysteresis observer is based on the Bouc-Wen model, the idea of high-order terminal sliding mode enhanced observer and the novel TSMC can be easily extended to other systems. In future work, we will try to transplant the algorithm to other systems. In addition, the control parameters in this paper are fixed parameters selected by trial-and-error method. The future direction of work will focus on developing adaptive strategy to automatically adjust the control parameters.

REFERENCES

[1] B. Mokaberi and A. A. G. Requicha, "Compensation of Scanner Creep and Hysteresis for AFM Nanomanipulation," *IEEE Trans. Autom. Sci. Eng.*, vol. 5, no. 2, pp. 197-206, Apr. 2008.

[2] T. Tang, S. xu Niu, T. Yang and B. Qi, "Suppressions of vibration in the tip-tilt mirror control system by add-on controller", *ISA Trans.*, vol. 102, pp. 245-250, Jul. 2020.

[3] M. Xie, S. Yu, H. Lin, J. Ma and H. Wu, "Improved Sliding Mode Control With Time Delay Estimation for Motion Tracking of Cell Puncture Mechanism," *IEEE Trans. Circuits Syst. I, Reg. Papers*, vol. 67, no. 9, pp. 3199-3210, Sep. 2020.

[4] S. Devasia, E. Eleftheriou and S. O. R. Moheimani, "A Survey of Control Issues in Nanopositioning," *IEEE Trans. Control Syst. Technol.*, vol. 15, no. 5, pp. 802-823, Sep. 2007.

[5] D. Liu, Y. Fang and H. Wang, "Intelligent Rate-Dependent Hysteresis Control Compensator Design With Bouc-Wen Model Based on RMSO for Piezoelectric Actuator," *IEEE Access*, vol. 8, pp. 63993-64001, 2020.

[6] G. Gu, L. Zhu, C. Su, H. Ding and S. Fatikow, "Modeling and Control of Piezo-Actuated Nanopositioning Stages: A Survey," *IEEE Trans. Autom. Sci. Eng.*, vol. 13, no. 1, pp. 313-332, Jan. 2016.

[7] Q. Xu, "Digital Integral Terminal Sliding Mode Predictive Control of Piezoelectric-Driven Motion System," *IEEE Trans. Ind. Electron.*, vol. 63, no. 6, pp. 3976-3984, Jun. 2016.

[8] S. Xiao and Y. Li, "Modeling and High Dynamic Compensating the Rate-Dependent Hysteresis of Piezoelectric Actuators via a Novel Modified Inverse Preisach Model," *IEEE Trans. Control Syst. Technol.*, vol. 21, no. 5, pp. 1549-1557, Sep. 2013.

[9] G. Gu, L. Zhu and C. Su, "Modeling and Compensation of Asymmetric Hysteresis Nonlinearity for Piezoceramic Actuators With a Modified Prandtl–Ishlinskii Model," *IEEE Trans. Ind. Electron.*, vol. 61, no. 3, pp. 1583-1595, Mar. 2014.

[10] C.-J. Lin, P.-T. Lin, "Tracking control of a biaxial piezo-actuated positioning stage using generalized duhem model," *Computers & Mathematics with Applications*, vol. 64, pp. 766-787, Sep. 2012.

[11] M. Rakotondrabe, "Bouc–Wen Modeling and Inverse Multiplicative Structure to Compensate Hysteresis Nonlinearity in Piezoelectric Actuators," *IEEE Trans. Autom. Sci. Eng.*, vol. 8, no. 2, pp. 428-431, Apr. 2011.

[12] Z. Nie, R. Liu, Q. Wang, D. Guo, Y. Ma, and Y. Lan. "Novel identification approach for nonlinear systems with hysteresis,". *Nonlinear Dynamics.*, vol. 95, no. 2, pp. 1053-66, Jan. 2019.

[13] M. H. M. Ramli, T. V. Minh and X. Chen, "Pseudoextended Bouc–Wen Model and Adaptive Control Design With Applications to Smart Actuators," *IEEE Trans. Control Syst. Technol.*, vol. 27, no. 5, pp. 2100-2109, Sep. 2019.

[14] P. Liu, P. Yan, Z. Zhang, T. Leng, "Modeling and control of a novel x–y parallel piezoelectric-actuator driven nanopositioner", *ISA Trans.*, vol. 56, pp. 145-154, May. 2015.

[15] X. Chen, C. Su, Z. Li and F. Yang, "Design of Implementable Adaptive Control for Micro/Nano Positioning System Driven by Piezoelectric Actuator," *IEEE Trans. Ind. Electron.*, vol. 63, no. 10, pp. 6471-6481, Oct. 2016.

[16] L. Cheng, W. Liu, C. Yang, T. Huang, Z. Hou and M. Tan, "A Neural-Network-Based Controller for Piezoelectric-Actuated Stick–Slip Devices," *IEEE Trans. Ind. Electron.*, vol. 65, no. 3, pp. 2598-2607, Mar. 2018.

[17] R. Xu and M. Zhou, "A self-adaption compensation control for hysteresis nonlinearity in piezo-actuated stages based on Pi-sigma fuzzy neural network," *Smart Mater. and Structures*, vol. 27, no. 4, pp. 045002, Feb. 2018.

[18] Y. Li and Q. Xu, "Adaptive Sliding Mode Control With Perturbation Estimation and PID Sliding Surface for Motion Tracking of a Piezo-Driven Micromanipulator," *IEEE Trans. Control Syst. Technol.*, vol. 18, no. 4, pp. 798-810, Jul. 2010.

[19] A. Šabanovic, "Variable Structure Systems With Sliding Modes in Motion Control—A Survey," *IEEE Trans. Ind. Informat.*, vol. 7, no. 2, pp. 212-223, May. 2011.

[20] C. Du, F. Li and C. Yang, "An Improved Homogeneous Polynomial Approach for Adaptive Sliding-Mode Control of Markov Jump Systems With Actuator Faults," *IEEE Trans. Autom. Control*, vol. 65, no. 3, pp. 955-969, March 2020.

[21] R. Xu, X. Zhang, H. Guo and M. Zhou, "Sliding Mode Tracking Control With Perturbation Estimation for Hysteresis Nonlinearity of Piezo-Actuated Stages," *IEEE Access*, vol. 6, pp. 30617-30629, 2018.

[22] S. Li, M. Zhou and X. Yu, "Design and Implementation of Terminal Sliding Mode Control Method for PMSM Speed Regulation System," *IEEE Trans. Ind. Informat.*, vol. 9, no. 4, pp. 1879-1891, Nov. 2013.

[23] H. Pan, W. Sun, H. Gao and J. Yu, "Finite-Time Stabilization for Vehicle Active Suspension Systems With Hard Constraints," *IEEE Trans. Intell. Transp. Syst.*, vol. 16, no. 5, pp. 2663-2672, Oct. 2015.

[24] F. Li, C. Du, C. Yang, L. Wu and W. Gui, "Finite-time asynchronous sliding mode control for Markovian jump systems," *Automatica*, vol. 109, pp. 108503, Nov. 2019.

[25] Y. Feng, X. Yu and F. Han, "High-Order Terminal Sliding-Mode Observer for Parameter Estimation of a Permanent-Magnet Synchronous Motor," *IEEE Trans. Ind. Electron.*, vol. 60, no. 10, pp. 4272-4280, Oct. 2013.
[26] Y. Shen, Y. Huang and J. Gu, "Global Finite-Time Observers for Lipschitz Nonlinear Systems," *IEEE Trans. Autom. Control*, vol. 56, no. 2, pp. 418-424, Feb. 2011.
[27] H. Pan and W. Sun, "Nonlinear Output Feedback Finite-Time Control for Vehicle Active Suspension Systems," *IEEE Trans. Ind. Informat.*, vol. 15, no. 4, pp. 2073-2082, April 2019.
[28] J. Wang, C. Zhang, S. Li, J. Yang and Q. Li, "Finite-Time Output Feedback Control for PWM-Based DC–DC Buck Power Converters of Current Sensorless Mode," *IEEE Trans. Control Syst. Technol.*, vol. 25, no. 4, pp. 1359-1371, July 2017.
[29] Man Zhihong and Xing Huo Yu, "Terminal sliding mode control of MIMO linear systems," *IEEE Trans. Circuits Syst. I, Fundam. Theory Appl*, vol. 44, no. 11, pp. 1065-1070, Nov. 1997.
[30] S. Li, X. Wang and L. Zhang, "Finite-Time Output Feedback Tracking Control for Autonomous Underwater Vehicles," *IEEE J. Ocean. Eng.*, vol. 40, no. 3, pp. 727-751, Jul. 2015.
[31] Y. Feng, X. Yu, Z. Man, "Non-singular terminal sliding mode control of rigid manipulators," *Automatica*, vol. 38, no. 12, pp. 2159-2167, Dec. 2002.
[32] A. Levant, "Chattering Analysis," *IEEE Trans. Autom. Control*, vol. 55, no. 6, pp. 1380-1389, June 2010.
[33] A. Safa, R. Y. Abdolmalaki and H. C. Nejad, "Precise Position Tracking Control With an Improved Transient Performance for a Linear Piezoelectric Ceramic Motor," *IEEE Trans. Ind. Electron.*, vol. 66, no. 4, pp. 3008-3018, April 2019.
[34] J. P. Mishra, Q. Xu, X. Yu and M. Jalili, "Precision Position Tracking for Piezoelectric-Driven Motion System Using Continuous Third-Order Sliding Mode Control," *IEEE/ASME Trans. Mechatronics*, vol. 23, no. 4, pp. 1521-1531, Aug. 2018.
[35] Y. Tian, Y. Cai and Y. Deng, "A Fast Nonsingular Terminal Sliding Mode Control Method for Nonlinear Systems With Fixed-Time Stability Guarantees," *IEEE Access*, vol. 8, pp. 60444-60454, 2020.
[36] D. Habineza, M. Rakotondrabe and Y. Le Gorrec, "Bouc–Wen Modeling and Feedforward Control of Multivariable Hysteresis in Piezoelectric Systems: Application to a 3-DoF Piezotube Scanner," *IEEE Trans. Control Syst. Technol.*, vol. 23, no. 5, pp. 1797-1806, Sep. 2015.
[37] V. Hassani, T. Tjahjowidodo and T. N. Do, "A survey on hysteresis modeling, identification and control," *Mechanical Systems and Signal Processing*, vol. 49, no. 1, pp. 209-233, Dec. 2014.
[38] X. S. Yang, "A new metaheuristic bat-inspired algorithm," in *Nature Inspired Cooperative Strategies for Optimization.* Berlin, Germany: Springer, 2010, pp. 65-74.
[39] Chiu C-S. "Derivative and integral terminal sliding mode control for a class of MIMO nonlinear systems," *Automatica*, vol. 48, no. 2, pp. 316-26, Feb. 2012.
[40] Z. Zhu, Y. Xia, and M. Fu, "Attitude stabilization of rigid spacecraft with finite-time convergence,*Int. J. Robust Nonlinear Control*, vol. 21, no. 6, pp. 686-702, 2011.
[41] F. Ikhouane, J. Rodellar, and A. Rodriguez, "Analytical study of the influence of the normalized Bouc-Wen model parameters on hysteresis loops," *Smart Structures and Materials*, R. C. Smith, Ed., vol. 5757 of Proceedings of SPIE, pp. 535–542, 2005.
[42] J.J.E. Slotine and W.Li., Applied Nonlinear Control, vol. 199. Englewood Cliffs, NJ, USA: Prentice-Hall, 1991.
[43] Q. Xu, "Digital Sliding Mode Prediction Control of Piezoelectric Micro/Nanopositioning System," *IEEE Trans. Control Syst. Technol.*, vol. 23, no. 1, pp. 297-304, Jan. 2015.

XIN CHE (S'18) received the B.S. degree from Jilin University, Changchun, China, in 2014.

He is currently pursuing the Ph.D. degree with Changchun Institute of Optics, Fine Mechanics and Physics, Chinese Academy of Sciences, Changchun, China. His research interests include nonlinear system control, variable structure control and advanced motion control.

DAPENG TIAN (S'10-M'13-SM'20) received the B.E. degree from Beijing Institute of Technology, Beijing, China, in 2007. He was then directly recommended to study at the Beijing University of Aeronautics and Astronautics (Beihang University), Beijing, where he received the Ph.D. degree in 2012. From 2009 to 2012, he was a Co-researcher with the Advanced Research Center, Keio University, Yokohama, Japan.

Since 2012, he has been with the Key Laboratory of Airborne Optical Imaging and Measurement, Changchun Institute of Optics, Fine Mechanics and Physics, Chinese Academy of Sciences, Changchun, China. He achieved the 2017's outstanding science and technology achievement prize of the Chinese Academy of Sciences and 2018's state science and technology award in China. His current research interests include motion control theory and engineering, optical imaging, and bilateral control.

RUI XU (M'20) received the Ph.D. degree in control theory and control engineering with the Department of Control Science and Engineering, Jilin University, Changchun, China, in 2019. From Sep. 2018 to Sep. 2019, he was an exchange PhD student with the Department of Electrical and Computer Engineering, Michigan State University, East Lansing, USA. Since 2020, he has been with the Key Laboratory of Airborne Optical Imaging and Measurement, Changchun Institute of Optics, Fine Mechanics and Physics, Chinese Academy of Sciences, Changchun, China.

His current research interests include Micro-nano drive control, motion control theory and optical imaging.

PING JIA received the B.E. degree from Jilin University of Technology, Changchun, Jilin, China, in 1981, the M.S. degree from University of Science and Technology of China, Hefei, Anhui, in 1985, and the P.hD. degree from Changchun Institute of Optics, Fine Mechanics and Physics, Chinese Academy of Sciences, Changchun, China.

He is currently the present of Changchun Institute of Optics, Fine Mechanics and Physics, Chinese Academy of Sciences, Changchun, China. He achieved dozens of awards including two times state science and technology award in China. He is the author of more than 50 articles and 19 inventions. His research interests include photoelectric imaging and measurement technology, image processing and high precision angle sensing technology.